Available online at www.worldnewsnaturalsciences.com

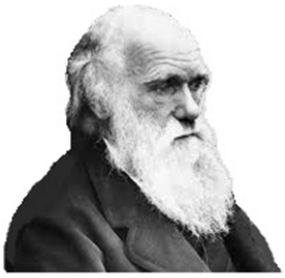

World News of Natural Sciences

An International Scientific Journal

WNOFNS 57 (2024) 100-118 EISSN 2543-5426

# Anti-corrosion and adsorption properties of 2-(2-Methyl-5-nitro-1H-imidazol-1-yl) ethanol: electrochemical and computational chemistry investigation

**Abima Julian Ogoba[1], Stephen Adie Adalikwu[1,2], Fidelis Ebunta Abeng[2,*], Alexander I. Ikeuba[3]**

[1] Department of Physics, Cross River State College of Education, Akamkpa, Cross River State, Nigeria

[2] Materials and Electrochemistry Research Group, Department of Chemistry, University of Cross River State. P. M. B. 1123, Calabar, Nigeria

[3] Materials Chemistry Research Group, Department of Pure and Applied Chemistry, University of Calabar, Calabar, Nigeria

*E-mail address: fidelisabeng@unicross.edu.ng

**ABSTRACT**

Because conventional inhibitors are nonbiodegradable and harmful, the development of eco-friendly corrosion inhibitors is gaining popularity. The anti-corrosive efficacy of 2-(2-Methyl-5-nitro-1H-imidazol-1-yl) ethanol on carbon steel in an chloride solution was evaluated in this study using a variety of approaches such as electrochemical measurements and computational studies. The results showed that increasing the concentration of 2-(2-Methyl-5-nitro-1H-imidazol-1-yl) ethanol from 0.1 to 3.0 g/L enhanced the inhibition efficiency (IE%) to 90.18-91.71 %. The high ΔE(eV) value of 0.239 and the interaction and binding energies of − 995.45 and 995.45 for 2-(2-Methyl-5-nitro-1H-imidazol-1-yl) ethanol molecules onto Fe (110) substrate were further supported by quantum chemical analytics, which also supported the empirical results. The results show that 2-(2-Methyl-5-nitro-1H-imidazol-1-yl) ethanol has a bright future as an effective and environmentally safe inhibitor for preventing carbon steel from corroding in corrosive media.

***Keywords*:** Carbon steel, Chloride solution, Electrochemical, DFT, MDS

( Received 22 August 2024; Accepted 27 September 2024; Date of Publication 29 September 2024 )

## 1. INTRODUCTION

In many industrial applications, carbon steel corrosion in chloride solution is still a major problem. Corrosion is a widespread issue that can lead to material loss and reduced mechanical capabilities [1-4]. The impact extends to industrial sectors, posing safety problems and significant economic costs. Carbon steel, a versatile material used in building, transportation, and manufacturing, is very susceptible to corrosion in aqueous environments like NaCl solution. Researchers have developed many techniques to protect mild steel from environmental corrosion, including the use of corrosion inhibitors. [4-8]. Corrosion of carbon steel in NaCl solutions can cause large economic losses and pose safety risks. Chloride solution is widely used in a variety of industries, such as metal production, chemical processing, and water treatment plants. Sadly, the widespread use of NaCl significantly increases the chance of corrosion in carbon steel structures and equipment, which can result in material deterioration and safety risks [9-12]. Let us introduce you to corrosion inhibitors, which are substances that work by creating a protective layer on the metal surface to stop or minimize corrosion by keeping corrosive substances out of the metal's weaker structural areas [13-18]. Inhibitors are classified as organic or inorganic based on chemical composition. Concerns about the toxicity and environmental impact of inorganic inhibitors, such as chromates and phosphates, have led to a growing interest in developing organic alternatives [19, 20].

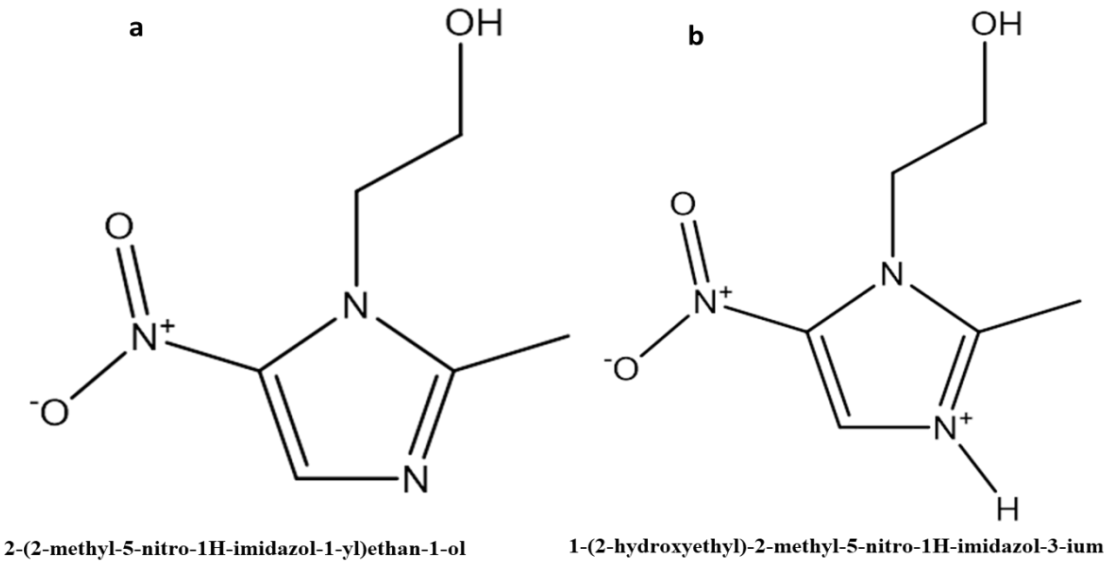


**Figure 1.** Molecular structure of metronidazole drug, MNZ (a) Neutral-MNZ and (b) Protonated-MNZ with Molecular formulae and Molar masses = $C_6H_9N_3O_3$, 171.16 g/mol and $[C_6H_{10}N_3O_3]^+$, 172.17 g/mol respectively

Nitrogen-, sulfur-, and oxygen-enriched organic compounds have drawn notice for their amazing inhibitory properties, which stem from their ability to create protective films on metal surfaces [21]. Many criteria, such as their chemical composition, adsorption behavior, and electrochemical characteristics, determine how effective organic inhibitors are; as a result, they

are classified into groups according to their structural traits, such as amines, quinolines, imidazoles, and azoles. Numerous kinds of organic compounds have been investigated and shown to be effective in inhibiting corrosion, including Schiff bases, pyridine derivatives, and benzotriazole derivatives [22-25]. This study aims to investigate 2-(2-Methyl-5-nitro-1H-imidazol-1-yl) ethanol potential as a corrosion inhibitor for carbon steel in NaCl solution considering this data. The study uses a variety of techniques, including theoretical and experimental approaches, to evaluate the efficacy of 2-(2-Methyl-5-nitro-1H-imidazol-1-yl) ethanol (Figure 1). Our goals are twofold: first, to provide insightful information about the possible use of 2-(2-Methyl-5-nitro-1H-imidazol-1-yl) ethanol as a carbon steel corrosion inhibitor in aqueous environment; and second, to obtain a thorough understanding of its mechanism of action.

## 2. EXPERIMENTAL

### 2. 1. Materials

The alloy that was used for this experiment was carbon steel, obtained from Department of Physics Mechanical Workshop, University of Calabar. The carbon steel sheets have a surface area of 1 $cm^2$ and are used as a working electrode. Their chemical composition of the steel recorded: Fe (99.93%), C (0.08%), Si (0.26%), Na (0.64%), S (0.05%), Ni (0.09%), Cr (0.08%), Mn (0.02%), and Cu (0.27%). After being abraded with emery paper with grit sizes ranging from 600 to 1000, the samples were dried in acetone, degreased in ethanol, and stored in a desiccator free of moisture. The 3.5 % NaCl corrosive medium was prepared using analytical grade reagents from Sigma-Aldrich. Distilled water was used to prepare each and every reagent.

#### 2. 1. 1. Preparation of stock solution of 2-(2-Methyl-5-nitro-1H-imidazol-1-yl) ethanol as inhibitor

3.0 g of 2-(2-Methyl-5-nitro-1H-imidazol-1-yl) ethanol powder was dissolved in 1000 mL of the 3.5% NaCl blank solution to create 3.0 g/L of the stock solution. To get 0.1 and 0.5 g/L, the 3.0 g/L stock solution was serially diluted. The corrosion test was conducted using these solutions at 303 K [26-28].

### 2. 2. Methods

#### 2. 2. 1. Electrochemical Measurement

Electrochemical testing in a three-electrode cell was carried out using a Gamry electrochemical workstation that was linked to a personal computer. The electrochemical cell's working electrode (WE) is a carbon steel sample, Saturated calomel electrodes (SCE) serve as the reference electrode (RE), whereas platinum electrodes serve as the auxiliary electrode (AE). After carbon steel was immersed in the test solution for five to ten minutes at 303K temperatures, the open circuit potential E was obtained [29-30]. There was a potential range of -250 mV to +250 mV. At a scan rate of 0.6 mV $sec^{-1}$, The current-potential curves of potentiodynamics were produced. EIS measurements were performed at the open circuit potential in the frequency ranges of 100 kHz and 0.01 Hz using small amplitude 10 mV AC pulses at 303K.

The impedance measurements were examined using a Nyquist plot. Studies were carried out in triplicate to calculate the % inhibition effectiveness, and the study with the best inhibition efficiency was published.

### 2. 2. 2. Density functional theory (DFT)/ Molecular dynamic simulation (MSD)

Quantum chemistry calculations were performed using a variation of Density Functional Theory (DFT) with the basis set B3LYP/6-3/G. The entire geometric optimization was completed by aqueous phase computations, demonstrating the relationship between the molecular characteristics of 2-(2-Methyl-5-nitro-1H-imidazol-1-yl) ethanol and its inhibitory potential. Figure 5a shows the compound's geometric configuration that maximizes least energy. Within the framework of the DFT theory, the energy levels of the highest occupied molecular orbital (EHOMO) and lowest unoccupied molecular orbital (ELUMO) were utilized to approximate the electron affinity (A) and ionization potential (I) supplied by Koopman's theorem. Using the energy of the lowest unoccupied molecular orbital (ELUMO) and highest occupied molecular orbital (EHOMO) energy values, the chemical potential and hardness that influence the atoms' resistance to the charge transfer process were determined, in compliance with the Koopmans theorem. The formula for determining the electrophilicity index (ω) can be found in Equation 10. The energy reduction brought about by the greatest amount of electron movement between the acceptor and donor is measured by the electrophilicity index (ω). Other quantum chemical properties like electronegativity (χ) and the proportion of transported electrons were also calculated. Equation 1 links variations in the external potential of the electron distribution V and the number of transferred electrons N to variations in electronic energy (dE) [31–33].

$$dE[p(r)] = \mu_p dN + \int p(r) dv(r) dr \quad (1)$$

The chemical potential was related to the first derivative of energy with regard to the number of electrons transferred; as a result, the electronegativity becomes negative according to equation 2 [33].

$$\mu_\rho = \left(\frac{E_{HOMO}+E_{LUMO}}{2}\right)_{v(r)} = \left(\frac{dE}{dN}\right)_{v(r)} - \chi \quad (2)$$

where V(r) is the system's external potential and is the electronic chemical potential, and E is the total energy and N is the number of electrons transported. The hardness η has been identified as the second partial derivative of the energy with regard to the number of electrons.

$$\eta = \mu_\rho = \left(\frac{E_{HOMO}-E_{LUMO}}{2}\right)_{v(r)} = -\chi \left(\frac{d^2E}{dN^2}\right)_{v(r)} = \left(\frac{d\mu_\rho}{dN}\right)_{v(r)} \quad (3)$$

The stability and reactivity of the molecule are evaluated by this formula [34]. Koopmans' theorem specifies the inhibitor's electron affinities (A) and ionization potential (I) as

$$I = -E_{Homo} \quad (4)$$

$$A = -E_{Lumo} \quad (5)$$

An atom or set of atoms' ability to draw electrons to itself is measured by their electronegativity (χ). This value can be obtained by applying Equation 6.

$$\chi = \frac{I+A}{2} \quad (6)$$

The chemical hardness (η) of an atom can be calculated using the following equation, which indicates its resistance to charge transfer.

$$\eta = \frac{I-A}{2} \quad (7)$$

The chemical softness (S) is calculated using equation 8, which is the inverse of hardness.

$$S = \frac{1}{\eta} = \frac{2}{I-A} \quad (8)$$

The fraction of electrons that were transferred from the inhibitor molecule to the metallic surface was calculated using equation 9:

$$\Delta N = \frac{\chi_m - \chi_{inh}}{2(\eta_m + \eta_{inh})} \quad (9)$$

where the electronegativity and hardness of the metal and the inhibitor are denoted by $(\chi_m \, with \, \eta_m)$ and $(\chi_{inh} \, with \, \eta_{inh})$, respectively. Hardness and electronegativity have theoretical values of $\chi_{Fe} = 7eV$ and $\eta_{Fe} = 0$, respectively. These numbers, along with the values indicated in Table 3, were used to compute the fraction of electrons transported [35-39].

$$\omega = \frac{\chi^2}{2\eta} \quad (10)$$

## 3. RESULTS AND DISCUSSION

### 3. 1. Electrochemical measurement results

The electrochemical impedance spectroscopy (EIS) technique is a valuable tool for investigating corrosion causes. This method was also used to investigate the effect of inhibitor concentration on the impedance behavior of carbon steel in a chloride solution.

The Nyquist form of the impedance data is shown in Figure 3a. According to the Nyquist plots, which show a depressed semi-circle with the center under the real axis as the concentration of 2-(2-Methyl-5-nitro-1H-imidazol-1-yl) ethanol rose, charge transfer is likely the main mechanism of corrosion [40–43]. Because of substrate roughness and solid surface inhomogeneities, solid electrodes have a depressed semicircle, also known as frequency dispersion [44]. 2-(2-Methyl-5-nitro-1H-imidazol-1-yl) ethanol has obviously altered the carbon steel's impedance response in the chloride solution. Figure 3b shows the same predicted pattern, with the low-frequency data of Log Z consistently increasing upon the addition of 2-(2-Methyl-5-nitro-1H-imidazol-1-yl) ethanol at each concentration under investigation. A wider signal in the inhibited solution has a phase angle of 75 degrees at the maximum

2-(2-Methyl-5-nitro-1H-imidazol-1-yl) ethanol concentration, and each semicircle in the phase angle plot (Figure 3c) likewise becomes symmetrical. Table 1 shows the impedance parameters that the Echem program calculated, such as solution resistance (Rs), charge transfer resistance (Rct), and maximum frequency (fmax). Inhibition efficiency (IE) values rise in proportion to 2-(2-Methyl-5-nitro-1H-imidazol-1-yl) ethanol concentration. Using the formula shown equation 11, the inhibition efficiency (% IE) was determined.

$$\% IE = \frac{R_{ct\ (inh)} - R_{ct(blank)}}{R_{ct\ (inh)}} \times 100 \quad (11)$$

where the charge transfer resistances for the inhibitor and blank solution are, respectively, $R_{ct\ (inh)}$ and $R_{ct\ (blank)}$. The double layer capacitance (Cdl) can be computed using the following equation:

$$C_{dl} = \frac{1}{2\pi \times R_{ct} \times f_{max}} \quad (12)$$

where fmax represents the maximum frequency shown in the Nyquist plot.

Based on the results in Table 1, the Rct values increased as the inhibitor concentration increased. Nevertheless, the value of Cdl decreases when the inhibitor's concentration increases. This can be explained by the decrease in the thickness of the electrical double layer and/or the local dielectric constant, indicating that 2-(2-Methyl-5-nitro-1H-imidazol-1-yl) ethanol functions by adsorption at the metal/solution interface [45-46]. The gradual replacement of water molecules on the electrode surface by 2-(2-Methyl-5-nitro-1H-imidazol-1-yl) ethanol molecules through adsorption may be the reason for the drop in Cdl values, as this decreases the degree of steel dissolving [47].

With and without the inhibitor, the carbon steel/solution interaction was simulated by fitting the obtained EIS data to Figure 2d, the electrical equivalent circuit. The circuit in use identifies both the solution resistance (Rs) and the charge transfer resistance (Rct). It is important to keep in mind that surface flaws affect the double layer capacitance (Cdl) value, which influences the constant phase element (CPE).

Solution resistance in the circuit is thought to be caused by the passive coating that developed on the steel surface. In order to provide some crucial insights into the kinetics of the anodic and cathodic reactions of the corrosion process, the Tafel polarization investigation was meticulously carried out.

Figure 2 shows the carbon steel polarization curves in a 3.5% NaCl solution, both with and without various concentrations of 2-(2-Methyl-5-nitro-1H-imidazol-1-yl) ethanol (0.00, 0.1 g/L, 0.5 g/L, and 3.0 g/L) at 303 K.

Table 2 presents the electrochemical parameters that were measured. These properties include the inhibition efficiency (IE%), anodic Tafel slope (βa), cathodic Tafel slope (βc), corrosion potential (Ecorr), and corrosion current density (icorr).

The acquired data demonstrate that, at constant temperature, the corrosion current density (icorr) reduces as 2-(2-Methyl-5-nitro-1H-imidazol-1-yl) ethanol concentration increases. One explanation for this behavior could be that as 2-(2-Methyl-5-nitro-1H-imidazol-1-yl) ethanol content increases in the reaction medium, more molecules of the inhibitor cling to the electrode surface, creating a protective coating that encompasses a greater surface area [48]. In light of

the determined values for the free corrosion current density, the inhibition efficiency was estimated using the following equation:

$$\% IE = 1 - \frac{j_{corr\,(inh)}}{j_{corr\,(blank)}} \times 100 \quad (13)$$

The corrosion current density for an inhibited solution is represented by $j_{corr\,(inh)}$ and for an uninhibited solution by $j_{corr\,(blank)}$. When 2-(2-Methyl-5-nitro-1H-imidazol-1-yl) ethanol is added as a corrosion inhibitor.

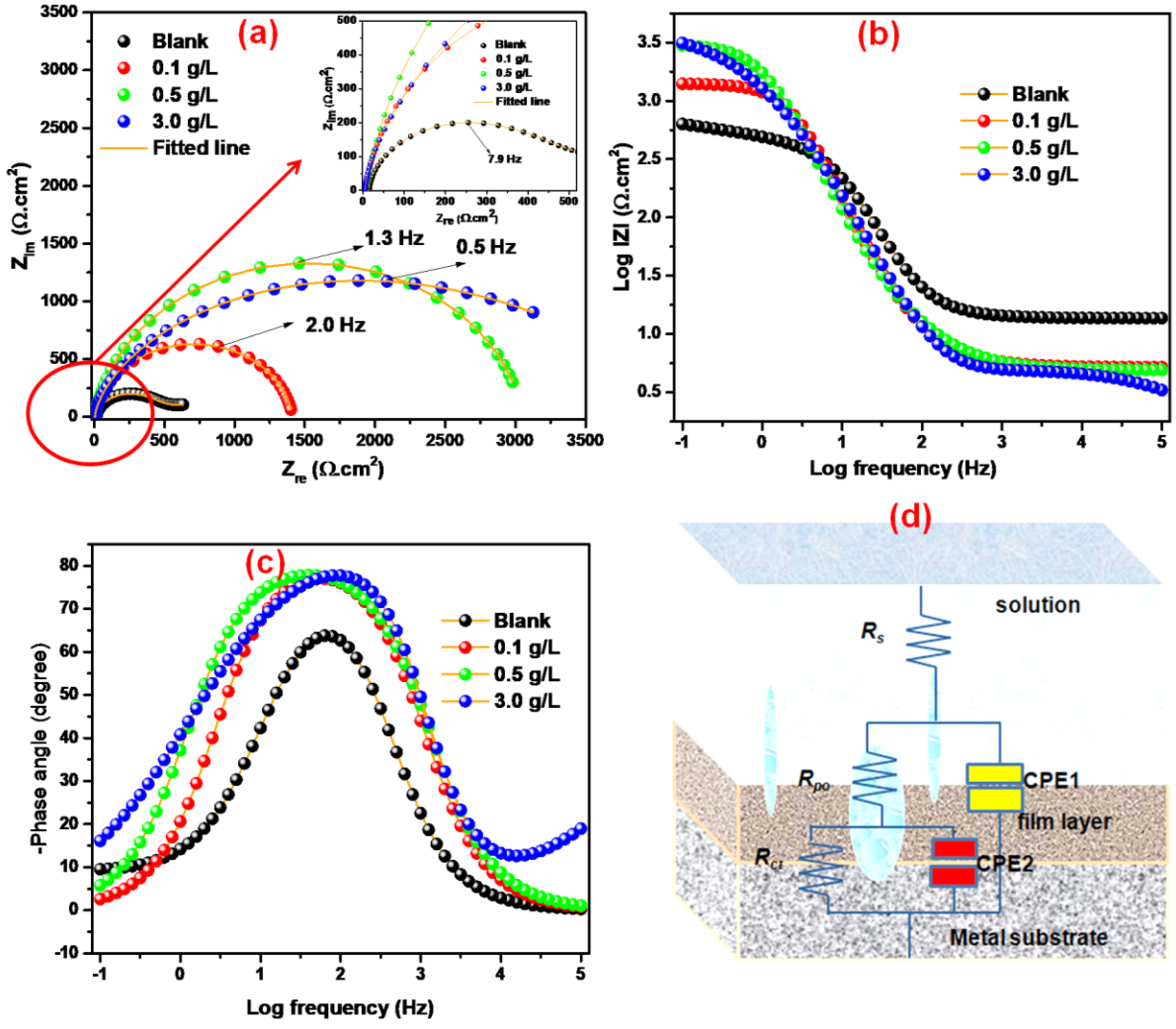


**Figure 2.** (**a**) Nyquist plots, (**b**) Frequency modulus, (**c**) Phase angle, (**d**) Equivalent circuit of carbon steel in blank 3.5 % NaCl and in varying concentration of 2-(2-Methyl-5-nitro-1H-imidazol-1-yl) ethanol.

Figure 3 demonstrates how the corrosion current densities at the open circuit potential (OCP) are dramatically altered, suggesting that carbon steel corrosion is significantly

suppressed. Based on the Ecorr departure from the blank solution, inhibitor compounds can be categorized as anodic, cathodic, or mixed-type, according to the literature [49-50]. If the displacement of Ecorr values in the presence and absence of inhibitors is greater than 85 mV, such an inhibitor molecules are generally classed as either cathodic or anodic; if the displacement of Ecorr values is less than 85 mV, they are referred to be mixed-type inhibitors [38].

**Table 1.** EIS data in the presence and absence of different concentrations of 2-(2-Methyl-5-nitro-1H-imidazol-1-yl) ethanol in 3.5 % NaCl solution at room temperature.

| System/ Conc. | $R_S$ ($\Omega \cdot cm^2$) | $CPE_1$ | | $R_{po}$ | $CPE_2$ | | $R_{ct}$ ($\Omega \cdot cm^2$) | $\chi^2$ ($\times 10^{-1}$) | $\eta_{EIS}$ (%) |
|---|---|---|---|---|---|---|---|---|---|
| | | $Y_{01}$($\times 10^{-5}$) ($\Omega^{-1} cm^{-2}$) | $n_1$ | | $Y_{02}$($\times 10^{-8}$) ($\Omega^{-1} cm^{-2}$) | $n_2$ | | | |
| **Blank** | 13.69 | 4.58 | 0.85 | 234.6± 0.41 | 26.75 | 0.8 | 343.50± 0.52 | 1.45 | - |
| **0.1 g/L** | 13.01 | 5.05 | 0.93 | 201± 0.74 | 10.48 | 0.90 | 1399± 0.67 | 1.11 | 63.94 |
| **0.5 g/L** | 13.12 | 4.97 | 0.92 | 603.8± 0.81 | 1.35 | 0.97 | 2943± 0.74 | 1.09 | 83.73 |
| **3.0 g/L** | 13.98 | 3.85 | 0.98 | 2874± 2.76 | 1.14 | 0.98 | 2999± 0.88 | 1.06 | 90.18 |

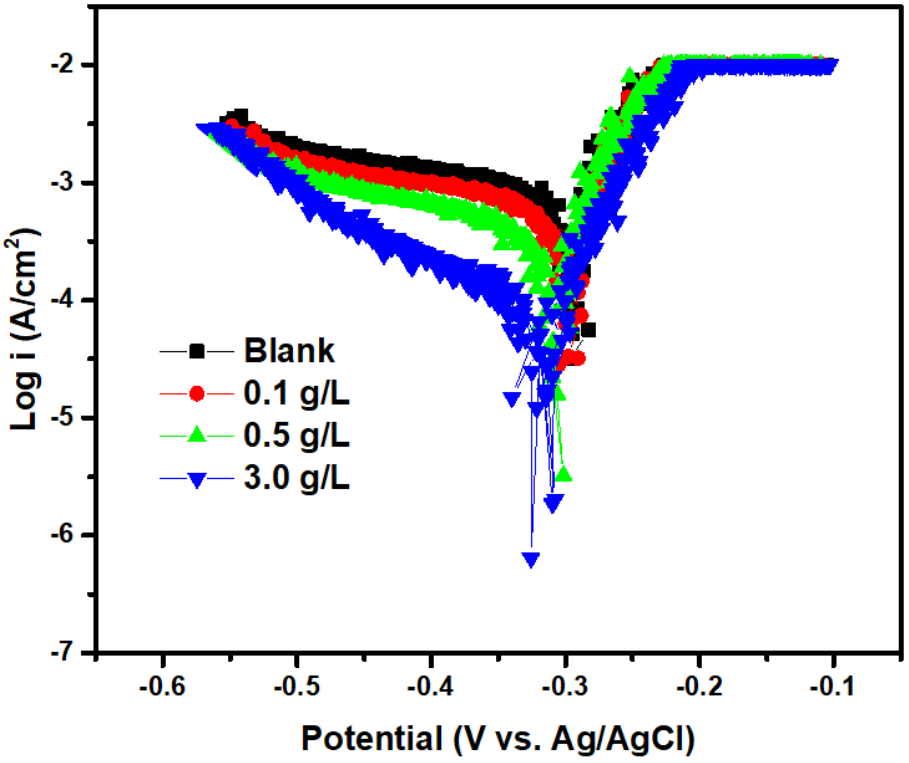


**Figure 3.** Polarization plots of carbon steel sample in 3.5 % NaCl solution in various concentration of 2-(2-Methyl-5-nitro-1H-imidazol-1-yl) ethanol.

**Table 2.** Potentiodynamic parameters in the presence and absence of different concentrations of 2-(2-Methyl-5-nitro-1H-imidazol-1-yl) ethanol in 3.5 % NaCl solution at room temperature.

| System/Conc. | $E_{corr}$ (mV vs. Ag/AgCl) | $i_{corr}$ (μA $cm^{-2}$) | $\beta_a$ (mV $dec^{-1}$) | $\beta_c$ (mV $dec^{-1}$) | $\eta_p$ % | $\theta$ |
|---|---|---|---|---|---|---|
| **Blank** | -285.80± 4.03 | 899.06± 1.81 | 163.44 | 89.81 | - | - |
| **0.1 g/L** | -298.66± 2.07 | 221.75± 1.72 | 86.64 | 76.45 | 75.33 | 0.75 |
| **0.5 g/L** | -301.61± 2.08 | 141.49± 0.98 | 73.75 | 68.37 | 84.27 | 0.84 |
| **3.0 g/L** | -303.61± 3.09 | 74.49± 0.98 | 56.84 | 64.22 | 91.71 | 0.91 |

### 3. 2. Density functional theory (DFT)

The frontier molecular orbital density distribution of the investigated 2-(2-Methyl-5-nitro-1H-imidazol-1-yl) ethanol molecule is shown in Figure 4. (HOMO and LUMO). The energy of EHOMO and ELUMO is crucial in determining the adsorption centers in the inhibitor's molecule, according to density functional theory. A higher adsorption is produced when empty d-orbital metals receive electron donations from the inhibitor molecules as EHOMO levels increases. Nevertheless, at lower ELUMO values, the inhibitor finds it easier to absorb an electron from a metal surface [51-52]. The efficiency of inhibition is influenced by the energy gap in the energy band (E = EHOMO - ELUMO). The energy gap (ΔE) is the amount of energy needed to extract an electron from the outer occupied orbital. Such molecules have poor inhibition performance when their energy gap (ΔE) and inhibitor's ionization potential are both large.

Furthermore, molecules with greater global hardness values are also more reactive, which reduces the compound's inhibitory efficacy [53-55]. The study's findings demonstrate a decreased value for both global hardness (η) and energy gap (ΔE), suggesting that the inhibitor under investigation performed well in terms of inhibitory efficiency. The dipole moment (μ) was used to assess the polarity of the covalent link between the investigated molecule and the metal surface. It is acknowledged that a high dipole moment (μ) value enhances the tested compound's adsorption tendency on the metal surface [56]. Considering the dipole moment (μ) value shown in Table 3,

The investigated chemical appears to have had good inhibitory performance. An effective corrosion inhibitor has the ability to donate electrons to the metal's vacant d-orbitals by removing free electrons from inhibitor molecules. As reactivity indices, the energies of the frontier molecular orbitals are employed. The dipole moment, ionization energy, electron affinity, and computed EHOMO and ELUMO values are all within the range of values reported for efficient corrosion inhibitors elsewhere [57]. Another crucial indicator of a chemical species is the electrophilicity index (ω). A good nucleophile is indicated by a small electrophilicity index value, whereas a high electrophilicity index value characterizes a good electrophile. According to my research, the study compound has a good ability to donate electrons to the metal surface, as shown by the electrophilicity index in Table 3 [58].

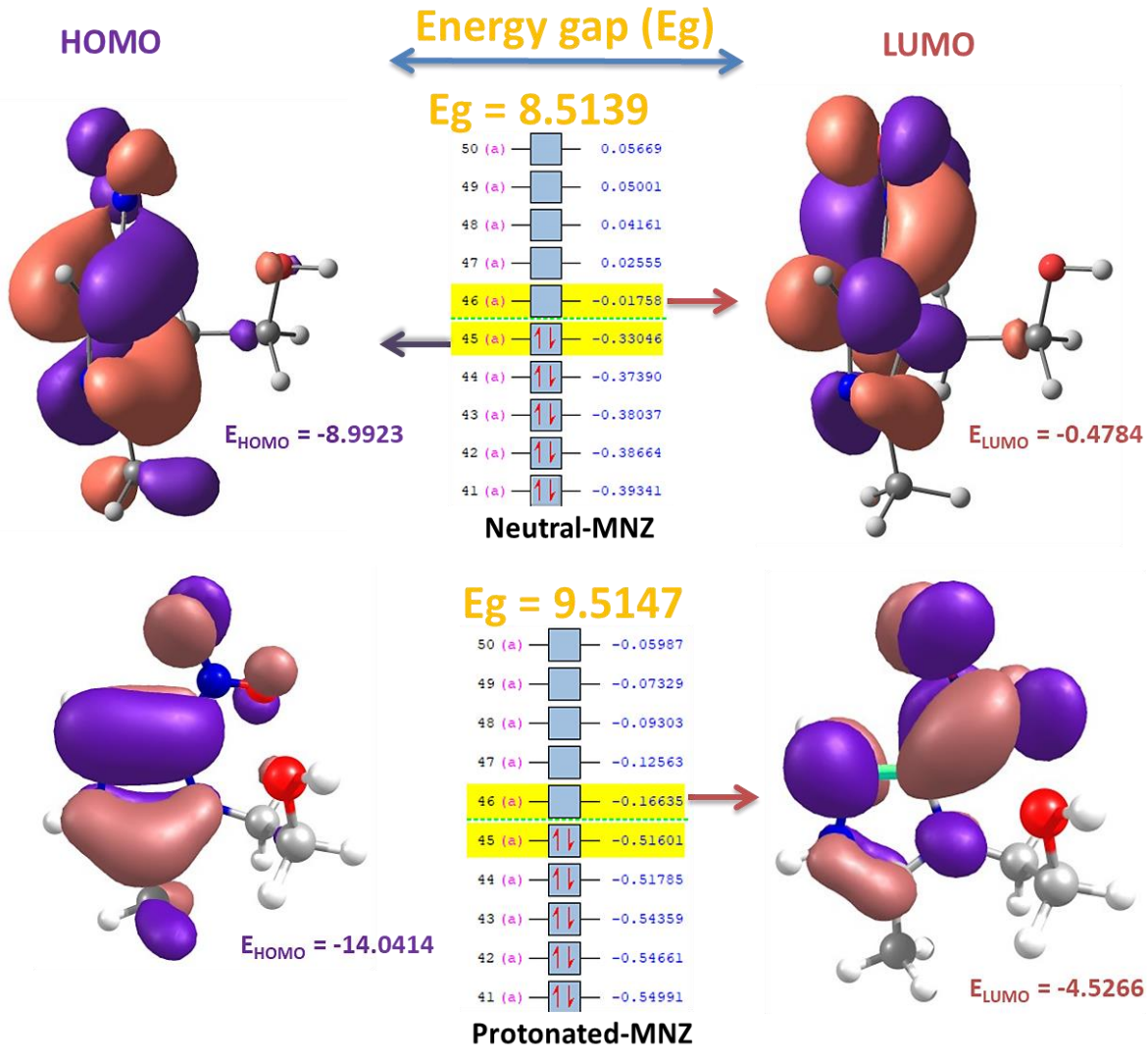


**Figure 4.** Frontier molecular orbitals showing HOMO and LUMO regions as well as the Energy gap.

**Table 3.** Ionization Potential (IP), Electron Affinity (EA), Electronegativity (χ), Chemical Potential (μ), Global Hardness (η), Global Softness (S) and Global Electrophilic Index (ω) of all investigated phases

| PHASE | IP (eV) | EA (eV) | χ (eV) | μ (eV) | η (eV) | α ($eV^{-1}$) | ω (eV) |
|---|---|---|---|---|---|---|---|
| N-MNZ | 8.9923 | 0.4784 | 9.2315 | -9.2315 | 8.7531 | 4.3764 | 19.4720 |
| P-MNZ | 14.0414 | 4.5266 | 16.3047 | -16.3047 | 11.7780 | 5.8890 | 45.1420 |

### 3. 3. Molecular Dynamics Simulation

Using the adsorption locator feature built into the Material Studio program, the Monte Carlo simulation technique was utilized to assist with the molecular simulation (from Accelerys Inc., 2020). Fe (110) was chosen to symbolize the mild steel crystal surface, where Fe basically makes up the majority of the composition. Introducing pure Fe crystal into the system and cleaving it into the Fe (110) surface, which is typically the most stable morphological surface with a low Miller index surface, is the initial stage in the simulation course. its favourable energetics and atomic density as compared to the Fe (111) and Fe (100).

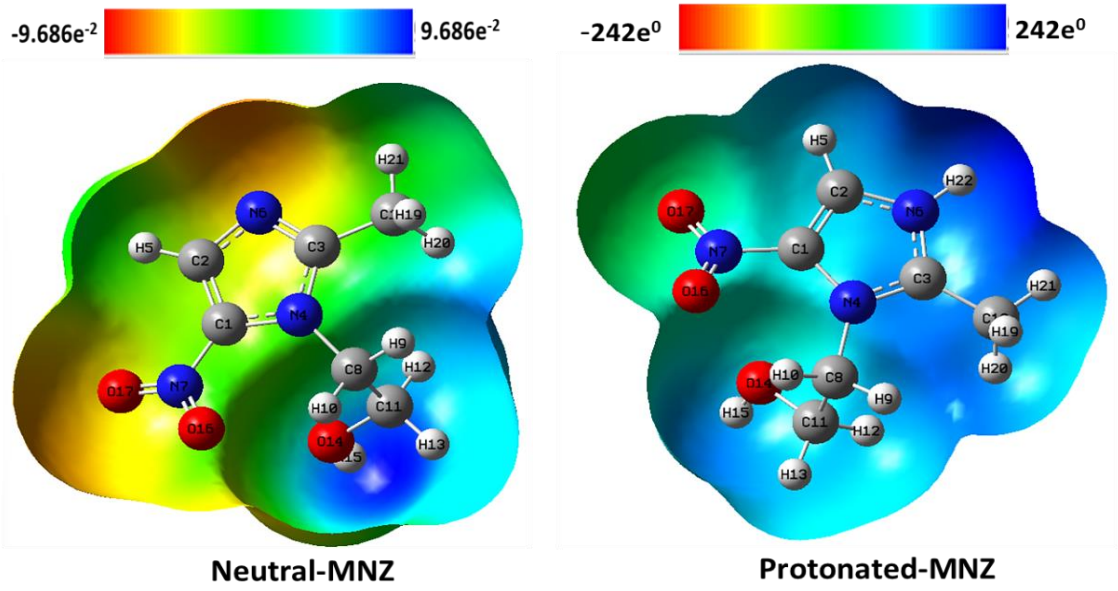


**Figure 5.** Molecular Electrostatic Potential (MESP) surfaces for the neutral and protonated phase of 2-(2-Methyl-5-nitro-1H-imidazol-1-yl) ethanol.

After importing the inhibitor into Materials Studio 2020 and sending them to DMoL3 for refinement of energy and shape, the Monte Carlo simulation was run in a simulation box of 24.2 × 24.2 × 42.1 Å3. Created with a vacuum block with a 20Å thickness. It was necessary to use the FORCEFIELD ASSIGNED charges and the COMPASS force field to optimize every system configuration in order to finish the simulation study. The computational configuration involved setting the displacement at $5 \times 10^{-5}$ Å with a maximum of 50 iterations, and the energy at $1 \times 10^{-4}$ kcal $mol^{-1}$ with a force of 0.005 kcal $mol^{-1}$ $Å^{-1}$. Atom-based van der Waals and electrostatic fields are both set to [59].

Molecular dynamic simulations are important for illuminating interacting adsorption processes or the interaction between inhibitors and surfaces. It is impossible to overlook the value of MD in gaining a comprehensive understanding of the surface chemistry and behavior of adsorbate molecules [60-61]. Based on these ideas, MD simulation has been utilized in this work to investigate the kind and mode of adsorption of the suggested corrosion inhibitor and consequently evaluate its effectiveness in preventing Fe corrosion. The adsorption configuration, adsorption energy, and adsorption mechanism of an inhibitor with changes in

adsorption temperature can all be used to determine how well it binds to and inhibits a corroded surface. Table 4 displays the interaction and equilibration energies of the inhibitor and complex, whereas Fig. 6 shows the two-dimensional representations of the inhibitor and surface interaction configurations. It can be deduced that the inhibitor attaches to the Fe surface efficiently based on the results of energy calculations.

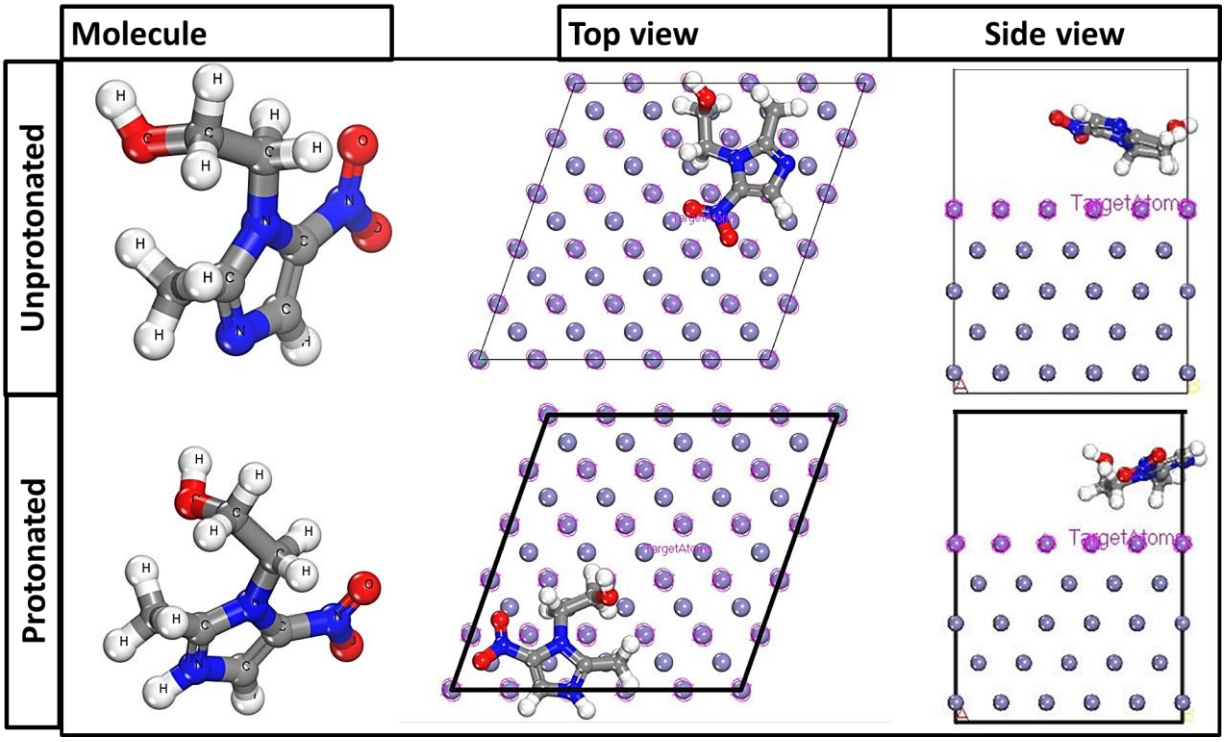


**Figure 6.** 2-(2-Methyl-5-nitro-1H-imidazol-1-yl) ethanol balance adsorption configurations on the Fe (110) surface in chloride solution at 298 K.

**Table 4.** Properties determined by the molecular simulation for the inhibitor molecules' adsorption on the Fe surface.

| Inhibitors | Inhibitor Energy (Kcal/mol) | MD simulation energy (Kcal/mol) | Interaction energy (Kcal/mol) |
|---|---|---|---|
| Neutral | -22.3559 | -21.0967 | -6.6608 |
| Protonated | 16.36 | 7.5463 | -8.8175 |

The neutral and protonated inhibitors showed favorable adsorption energies of -6.6608 and -8.8175 kcal/mol, respectively. The adsorption configuration, adsorption energy, and adsorption mechanism of an inhibitor with changes in adsorption temperature can all be used

to determine how well it binds to and inhibits a corroded surface. Table 4 displays the interaction and equilibration energies of the inhibitor and complex, whereas Fig. 6 shows the two-dimensional representations of the inhibitor and surface interaction configurations. It can be deduced that the inhibitor attaches to the Fe surface efficiently based on the results of energy calculations [63-66].

## 4. CONCLUSIONS

2-(2-Methyl-5-nitro-1H-imidazol-1-yl) ethanol corrosion-inhibiting effectiveness on carbon steel in 3.5 % NaCl was estimated in this study using a Electrochemical measurement and computational approach. The following is a summary of the main conclusions drawn from these experiments:

1). At 3.0 g/L and 298 K, 2-(2-Methyl-5-nitro-1H-imidazol-1-yl) ethanol was found to have a good IE% of 91 %, indicating that it can be employed in substantial quantities to provide extensive corrosion protection. Industries may be able to reduce the frequency of maintenance and repair by utilizing 2-(2-Methyl-5-nitro-1H-imidazol-1-yl) ethanol as a corrosion inhibitor, which could result in cost savings.

2). By examining the PDP slopes in 2-(2-Methyl-5-nitro-1H-imidazol-1-yl) ethanol and chloride solutions, 2-(2-Methyl-5-nitro-1H-imidazol-1-yl) ethanol has been determined to be a mixed-type corrosion inhibitor on the cathode. Significant corrosion inhibition potential was indicated by the sharp declines in the icorr values from 899.06 to 74.49 (μA) that occurred with increasing 2-(2-Methyl-5-nitro-1H-imidazol-1-yl) ethanol concentrations (01–3.0 g/g).

3). According to quantum chemical calculations, the components of the 2-(2-Methyl-5-nitro-1H-imidazol-1-yl) ethanol has a major effect on preventing corrosion in carbon steel. The synergistic effect of molecules on Fe (110) has the highest ΔE (eV) value of 0.239 and the values for $E_{interaction}$ and $E_{binding}$ are – 8.318 and -16.36, respectively.

**Funding:** The trust fund for tertiary education in Nigeria (Tetfund) provided funding for this study.

**Acknowledgments**

The authors extend their appreciation to the tertiary education trust fund (Tetfund) for funding this research through institution based research (IBR).

## References

[1] N. Arrousse, R. Salim, A. Abdellaoui, F. El Hajjaji, B. Hammouti, El Houssine M, W. Agerico Diño, M. Taleb, Synthesis, characterization, and evaluation of xanthene derivative as highly effective, nontoxic corrosion inhibitor for mild steel immersed in 1 M HCl solution. *J. Taiwan Inst. Chem. Eng.* 2021; 120: 344–359

[2] M. G. Mohamed, A. Mahdi, R. J. Obaid, M. A. Hegazi, S. W. Kuo, K. I. Aly, Synthesis and characterization of polybenzoxazine/clay hybrid nanocomposites for UV light shielding and anti-corrosion coatings on mild steel, *J. Poly. Res.* 2021; 28: 264-276

[3] M. G. Mohamed, S. W. Kuo, A. Mahdi, I. M. Ghayd, K. I. Aly, Bisbenzylidene cyclopentanone and cyclohexanone-functionalized polybenzoxazine nanocomposites: Synthesis, characterization, and use for corrosion protection on mild steel. *Mater. Today Comm.* 2020; 25: 101418

[4] K. I. Aly, A. Mahdi, M. A. Hegazi, N. S. Al-Muaikel, S. W. Kuo, M. G. Mohamed, Corrosion resistance of mild steel coated with Phthalimide-Functionalized polybenzoxazines. *Coating.* 2020 a, 10 (11), 1114

[5] K. I. Aly, M. G. Mohamed, O. Younis, M. H. Mahross, M. A. Hakim, M. M. Sayed, Salicylaldehyde azine-functionalized polybenzoxazine: synthesis, characterization, and its nanocomposites as coatings for inhibiting the mild steel corrosion. *Prog. Org. Coat*. 2020b; 138: 105385

[6] K. I. Aly, O. Younis, M. H. Mahross,O. Tsutsumi, M. G. Mohamed, M. M. Sayed, Novel conducting polymeric nanocomposites embedded with nanoclay: synthesis, photoluminescence, and corrosion protection performance. *Poly. J.* 2019; 51: 77-90

[7] M. Zunita, Y. J. Kevin, Ionic liquids as corrosion inhibitor: From research and development to commercialization. *Results in Eng.* 15 (2022) 100562

[8] A. A. Ayoola, R. Babalola, B. M. Durodola, E. E. Alagbe, O. Agboola, E. O. Adegbile, Corrosion inhibition of A36 mild steel in 0.5 M acid medium using waste citrus limonum peels. *Results in Eng.* 15(2022) 100490

[9] M. A. Quraishi, D. S. Chauhan, Drugs as environmentally sustainable corrosion inhibitors: Sustainable corrosion inhibitors II: Synthesis, design, and practical applications ACS symposium series; American Chemical Society: Washington, DC, 2021

[10] I. B. Obot, E. E. Ebenso, M M. Kabanda, Metronidazole as environmentally safe corrosion inhibitor for mild steel in 0.5 M HCl: Experimental and Theoretical Investigation. *J. Environ. Chem. Eng.* 2013, 1 (3), 431–439

[11] I. B. Obot, I. B. Onyeachu, S. A. Umoren, S. A. Alternative corrosion inhibitor formulation for carbon steel in $CO_2$-saturated brine solution under high turbulent flow condition for use in oil and gas transportation pipelines. Corros. Sci. 159 (2019) 108140

[12] I. B. Onyeachu, I. B. Obot, A. Y. Adesina, Green corrosion inhibitor for oilfield application Ii: The time–evolution effect on the sweet corrosion of API X60 steel in synthetic brine and the inhibition performance of 2-(2-Pyridyl) benzimidazole under turbulent hydrodynamics. *Corros. Sci.* 2020, (2020), 108589

[13] Hossain, N., Asaduzzaman Chowdhury, M., & Kchaou, M. (2020). An overview of green corrosion inhibitors for sustainable and environment friendly industrial development. *Journal of Adhesion Science and Technology*, 35(7), 673–690. https://doi.org/10.1080/01694243.2020.1816793

[14] M. A. Quraishi, D. S. Chauhan, V. S. Saji, Heterocyclic organic corrosion inhibitors: principles and applications; Elsevier Inc: Amsterdam, 2020.

[15] N. Y. Diki, N. H. Coulibaly, O. Kambire, A. Trokoourey, Experimental and theoretical investigation on copper corrosion inhibition by cefixime drug in 1 M $HNO_3$ solution. *J. Mater. Sci. Chem. Eng*. 9 (2021) 11–28

[16] N. Y. Diki, N. H. Coulibaly, J. N. Yao, A. Trokourey, Thermodynamic and DFT studies on the behavior of cefadroxil drug as effective corrosion inhibitor of copper in one molar nitric acid medium. *J. Mater. Env. Sci.* 2019; 10 (10): 926–938.

[17] A. Ouedraogo, N. Y. Diki, B. W. Irie, N. H. Coulibaly, A. Trokourey, Copper corrosion inhibition by cefpodoxime drug in 1M Nitric Acid: Experimental and DFT approaches. *Int. J. Innov. Appl. Stud.* 2018; 24 (3): 1299–1311

[18] Y. S. Brou, N. H. Coulibaly, N. Y. Diki, J. Creus, A. Trokourey, Electrochemical study of the synergistic effect of two copper corrosion inhibitors, nicotinic acid and nicotina amide in two different media. *Open J. Phys. Chem.* 2019, 9: 193–203

[19] M. A. Tigori, P. M. Niamien, A. Trokourey, Thiamine hydrochloride as copper corrosion inhibitor in 1 M $HNO_3$. *J. Prog. Chem.* 2016, 4 (1)166–178.

[20] B. M. Prasanna, B. M. Praveen, N. Hebbar, M. K. Pavithra, T. S. Manjunatha, R. S. Malladi, Theoretical and Experimental approach of inhibition effect by sulfamethoxazole on mild steel corrosion in 1 M HCl. Surf. Inter. Analysis, 2018; 50 (8): 779–789

[21] F. E. Abeng**,** V.C. Anadebe, V.D. Idim, M.M. Edim. Anti-corrosion behaviour of expired tobramycin drug on carbon steel in acidic medium, S. Afr. J. Chem. 2020; 73: 125–130

[22] N. H. Coulibaly, Y. S. Brou, S. Akpa, C. Juan, A. Trokourey. Nicotinamide inhibition properties for copper corrosion in 3.5 % NaCl solution: Experimental and theoretical Investigation. *J. Mate. Sci. Chem. Eng.* 2018; 6: 100–121

[23] A. Ouedrogo, N. Y. Diki, K. V. Bohoussou, D. Soro, A. Trokourey. Copper corrosion inhibition by cefuroxime drug in 1 M nitric acid. *Chem. Sci. Rev. Lett.* 2018; 7 (26) 427–437

[24] V.C. Anadebe, O.D. Onukwuli, M. Omotioma, N.A. Okafor, Experimental, theoretical modeling and optimization of inhibition efficiency of pigeon pea leaf extract as anti-corrosion agent of mild steel in acid environment. *Mater Chem. Phys.* 2019; 233: 120-132

[25] T. Yan, S. Zhang, L. Feng, Y. Qiang, L. Lu, D. Fu, Y. Wen, J. Chen, W. Li, B. Tan, Investigation of imidazole derivatives as corrosion inhibitors of copper in sulfuric acid: combination of experimental and theoretical researches, *J. Taiwan Inst. Chem. Eng.* 2020; 106: 118–129

[26] V.C. Anadebe, C.S. Okafor, O.D. Onukwuli, Electrochemical, molecular dynamics, adsorption studies and anti-corrosion activities of moringa leaf biomolecules on carbon steel surface in alkaline and acid environment. *Chemical Data Collection.* 2020; 28: 100437

[27] S, Attabi, M. Mokhtari, Y. Taibi, I. Abdel-Rahman, B. Hafez, H. Elmsellem, Electrochemical and Tribological Behavior of Surface-Treated Titanium Alloy Ti-6Al-4V. *Journal of Bio-and Tribo-Corrosion*, 5 (2019), 2

[28] T. E. Gber, H. Louis, A. E. Owen, B. E. Etinwa, I. Benjamin, F. C. Asogwa, E. A. Eno, E. A. Heteroatoms (Si, B, N, and P) doped 2D monolayer MoS2 for $NH_3$ gas detection. *RSC Advances*, 2022, 12 (40) 25992-26010

[29] A. Liu, W. Guan, X. Zhao, X. Ren, X. Liang, L. Gao, T. Ma, Investigation on the interfacial behavior of polyorganic inhibitors on a metal surface by DFT study and MD simulation. *Appl. Surf. Sci.* 541 (2021) 148570

[30] A. Kokalj, On the alleged importance of the molecular electron-donating ability and the HOMO–LUMO gap in corrosion inhibition studies. *Corros. Sci.* 180 (2021) 109016

[31] S. A. Adalikwu, H. Louis, H. O. Edet, I. Benjamin, T. C. Egemonye, E. A. Eno, A.S. Adeyinka, Detection of hydrogen fluoride (HF) gas by $Mg_{12}O_{11}$-X (X= S, P, N, and B) nanosurfaces. *Chemical Physics Impact*, 5 (2022) 100129.

[32] A. I. Ikeuba, A. U. Agobi, L. Hitler, B. J. Omang, F. C. Asogwa, I. Benjamin, M. C. Udoinyang, M. C. Green Approach towards corrosion inhibition of mild steel during acid pickling using chlorpheniramine: Experimental and DFT Study. *Chemistry Africa*, 2022, 1-15

[33] H. Louis, M. Patrick, I. O. Amodu, I. Benjamin, I. J. Ikot, G. E. Iniama, A. S. Adeyinka, Sensor behavior of transition-metals (X = Ag, Au, Pd, and Pt) doped Zn11-X- $O_{12}$ nanostructured materials for the detection of serotonin. *Materials Today Communications*, 34 (2023) 105048

[34] D. Daouda, T. Douadi, D. Ghobrini, N. Lahouel,H. Hamani, Investigation of some phenolic-type antioxidants compounds extracted from biodiesel as green natural corrosion inhibitors;DFT and molecular dynamic simulation, comparative study. In *AIP Conference Proceedings*, 2019, Vol. 2190, No.1, page 020098

[35] E. A. Eno, C. R. Cheng, H. Louis, T E. Gber, W. Emori, I. A. T. Ita, A. S. Adeyinka, Investigation on the molecular, electronic and spectroscopic properties of rosmarinic acid: an intuition from an experimental and computational perspective. *Journal of Biomolecular Structure and Dynamics*, 2022, 1-15

[36] C. G. Apebende, H. Louis, A. E. Owen, I. Benjamin, I. O. Amodu, T. E. Gber, F. C. Asogwa, Adsorption properties of metal functionalized fullerene ($C_{59}Au$, $C_{59}Hf$, $C_{59}Ag$, and $C_{59}Ir$) nanoclusters for application as a biosensor for hydroxyurea (HXU): insight from theoretical computation. *Zeitschrift für Physikalische Chemie*, 2022, **236** (11-12), 1515-1546

[37] H. Louis, J. F. Eze, D. N. Adanna, H. O. Edet, T. O. Unimuke, E. A. Eno, V. N. Osabor, A. S. Adeyinka. Computational study of the interaction of c12p12 and c12n12 nanocages with alendronate drug molecule. *Chemistry Select* 8, (1) (2023) e202203607

[38] A. Liu, W. Guan, X. Zhao, X. Ren, X. Liang, L. Gao, T. Ma, Investigation on the interfacial behavior of polyorganic inhibitors on a metal surface by DFT study and MD simulation. *Appl. Surf. Sci.* 541 (2021) 148570

[39] M, Abdallah, K. A. Soliman, M. Alshareef, A. S. Al-Gorair, H. Hawsawi, H. M. Altass, M. S. Motawea, Investigation of the anticorrosion and adsorption properties of two polymer compounds on the corrosion of SABIC iron in 1 M HCl solution by practical and computational approaches. *RSC Advances*, 2022, 12 (31), 20122-20137

[40] F.O. Edoziuno, A.A. Adediran, B.U. Odoni, C.C. Nwaeju, O.S. Adesina, M. Oki, Influence of wormin mebendazole on the corrosion of mild steel in 1.0 M sulfuric acid. *Results in Eng.* 9 (2021) 100192

[41] H. Lgaz, S. K. Saha, A. Chaouiki, K. S. Bhat, R. Salghi, Shubhalaxmi, P. Banerjee, I. H. Ali, M. I. Khan, I. Chung, Exploring the potential role of pyrazoline derivatives in corrosion inhibition of mild steel in hydrochloric acid solution: Insights from experimental and computational studies. *Const. Build. Mater.* 233 (2020), 117320.

[42] S. Nikpour, M. Ramezanzadeh, G. Bahlakeh, B. Ramezanzadeh, M. Mahdavian, Eriobotrya japonica Lindl leaves extract application for effective corrosion mitigation of mild steel in HCl solution: experimental and computational studies. *Const. Build. Mater*. 220 (2019) 161-176

[43] F. E. Abeng, M. E. Ikpi, O. A. Ushie, V. C. Anadebe, B. E. Nyong, M. E. Obeten, N. A. Okafor, V. I. Chukwuike, P. Y. Nkom. Insight into corrosion inhibition mechanism of carbon steel in 2 M HCl electrolyte by eco-friendly based pharmaceutical drugs. *Chem. Data Collection* 2021; 34: 100722

[44] V. C. Anadebe, O. D. Onukwuli, F. E. Abeng, N. A. Okafor, J.O. Ezeugo, C. C. Okoye, Electrochemical-kinetics, MD-simulation and multi-input single-output (MISO) Modeling using adaptive neuro-fuzzy interference system (ANFIS) prediction for dexamethasone drug as eco-friendly corrosion inhibitor for mild steel in 2 M HCl electrolyte. *J. Taiwan Inst. Chem. Eng*. 2020; 115: 251–265

[45] A. Jasim, K. H. Rashid, K. F. AL-Azawi, A. A. Khadom, Synthesis of a novel pyrazole heterocyclic derivative as corrosion inhibitor for low-carbon steel in 1M HCl: Characterization, gravimetrical, electrochemical, mathematical, and quantum chemical investigations, *Result in Eng*. 15 (2022) 100573

[46] A. A. Khadom, A. A. Mahmmod, Quantum chemical and mathematical statistical calculations of phenyltetrazole derivatives as corrosion inhibitors for mild steel in acidic solution: A theoretical approach, *Result in Eng*. 16 (2022) 100741

[47] O. Oyewole, T.S. Abayomi, T. A. Oreofe, T. A. Oshin, Anti-corrosion using rice straw extract for mild steel in 1.5 M H2SO4 solution, *Result in Eng.* 16 (2022) 100684

[48] O. Sanni, J. Ren, T. Jen, Agro-industrial wastes as corrosion inhibitor for 2024-T3 aluminum alloy in hydrochloric acid medium. *Result in Eng.* 16 (2022) 100676

[49] T. Sithuba, N. D. Masia, J. Moema, L. C. Murulana, G. Masuku, I. Bahadur, M. M. Kabanda, Corrosion inhibitory potential of selected flavonoid derivatives: Electrochemical, molecular Zn surface interactions and quantum chemical approaches. *Result in Eng.* 16 (2022) 100694

[50] A.A. Ayoola, B.M. Durodola, R. Babalola, O.D. Adeniyi, C.E. Ilobinso, Corrosion inhibitive effects of calcium-modified zinc phosphate coating on A36 mild steel. *Result in Eng.* 17 (2023) 100880

[51] M. Beniken, R. Salim, E. Ech-chihbi, M. Sfaira, B. Hammouti, M. E. Touhami, M. A. Mohsin, M. Hammouti, M. Taleb. Adsorption behavior and corrosion inhibition mechanism of a polyacrylamide on C-steel in 0.5 M H2SO4. Electrochemical assessment and molecular dynamic simulations. *J. Mol. Liq.* 2021. 118022

[52] V. Kalia, P. Kumar, S. Kumar, M. Goyel, P. Pahuja, G. Jhaa, S. Lata, H. Dahiya, A. Kumari, C. Verma, Sythesis, characterization and corrosion inhibition potential of Oxadiazole derivatives for mild steel in HCl: Electrochemical and Computational studies. *J. Mol. Liq.* 2021; 118021

[53] H. Elmsellem, Y. El Ouadi, M. Mokhtari, H. Bendaif, H. Steli, A. Aouniti, A. M. Almehdi, I. Abdel-Rahman, HH. S. Kusuma, B. Hammouti. A natural antioxidant and an environmentally friendly inhibitor of mild steel corrosion: a commercial oil of basil (Ocimum basilicum l.). *J. Chem. Tech. Metall.* 4 (2019) 742-749

[54] F. Yousfi, H. Elmsellem, G. Fekkar, M. Aiboudi, M. Ramdani, I. Abdel-Rahman, B. Hammouti, L. Bouyazza, Eco-friendly Chamaerops humilis L. fruit extract corrosion inhibitor for mild steel in 1 M HCl. *Int. J. Corros. Scale Inhibition.* 9 (2020) 446-459

[55] B. Hafez, M. Mokhtari, H. Elmsellem, H. Steli, Environmentally friendly inhibitor of the corrosion of mild steel: Commercial oil of Eucalyptus. *Int. J. Corros. Scale Inhibition* 8 (2019) 573-585

[56] H. Elmsellem, T. Harit, A. Aouniti, F. Malek, A. Riahi, A. Chetouani, B. Hammouti, Adsorption properties and inhibition of mild steel corrosion in 1 M HCl solution by some bipyrazolic derivatives: experimental and theoretical investigations, Protection of Metals and Physical Chemistry of Surfaces 51 (2015) 873-884

[57] K. Chkirate, K. Azgaou, H. Elmsellem, et al., Corrosion inhibition potential of 2-[(5-methylpyrazol-3-yl) methyl] benzimidazole against carbon steel corrosion in 1 M HCl solution: Combining experimental and theoretical studies. *J Mol. Liq.* 321 (2021) 114750

[58] M. Yadav, R. R. Sinha, T. K. Sarkar, I. Bahadur, E. E. Ebenso, Application of new isonicotinamides as a corrosion inhibitor on mild steel in acidic medium: Electrochemical, SEM, EDX, AFM and DFT investigations. *J. Mol. Liq.* 212 (2015) 686–698

[59] H. Elmsellem, H. Nacer, F. Halaimia, A. Aouniti, I. Lakehal, A. Chetouani, S. S. Al-Deyab, R. Touzani, B. Hammouti, Anti-corrosive Properties and Quantum Chemical Study of (E)- 4-Methoxy-N-(Methoxybenzylidene) Aniline and (E)-N-(4-Methoxybenzylidene)-4-Nitroaniline Coating on Mild Steel in Molar Hydrochloric. *Int. J. Electrochem. Sci.* 9 (2014) 5328

[60] K. Azgaou, M. Damej, S. El Hajjaji, N. Kheira Sebbar, H. Elmsellem, B. El Ibrahimi, M. Benmessaoud, Synthesis and characterization of N-(2-aminophenyl)-2-(5-methyl-1H-pyrazol-3-yl) acetamide (AMPA) and its use as a corrosion inhibitor for C38 steel in 1 M HCl. Experimental and theoretical study. *J. Mol. Str.* 1266 (2022) 133451

[61] L. Toukal, D. Belfennache, M. Foudia, R. Yekhlef, F. Benghanem, B. Hafez, H. Elmsellem, I. Abdel-Rahman, Inhibitory power of N,N′-(1,4-phenylene)bis(1 (4nitrophenyl) methanimine) and the effect of the addition of potassium iodide on the corrosion inhibition of XC70 steel in HCl medium: Theoretical and experimental studies. *Int. J. Corros. Scale Inhibition.* 11 (2022) 438-464

[62] B. Tan, S. Zhang, H. Liu, Y. Guo, Y. Qiang,W. Li, L. Guo, C. Xu, S. Chen, Corrosion inhibition of X65 steel in sulfuric acid by two food flavorants 2-isobutylthiazole and 1(1,3-Thiazol-2-yl) ethanone as the green environmental corrosion inhibitors: combination of experimental and theoretical researches. *J. Coll. Inter. Sci.* (2019) 538: 519–529

[63] I. Danaee, S. R. Kumar, M. R. Avei, M. Vijayan, Electrochemical and Quantum chemical Studies on corrosion inhibition performance of 2, 2-(2-hydroxyethylimino)bis[N-(alphaalpha-dimethylphenethyl)-N-methylacetamide] on mild steel corrosion in 1 M HCl solution. *Mater. Res.* 23 (2020) e20180610

[64] M. Abdallah, E. A. M. Gad, M. Sobhi, J. H. Fahemi, M. M. Alfakeer, Performance of Tramadol drug as safe inhibitor for Aluminum corrosion in 1.0 M HCl solution and understanding mechanism of inhibition using DFT. *Egypt. J. Petr.* 28 (2019) 173–181

[65] D. Douche, H. Elmsellem, E. H. Anouar, et al., Anti-corrosion performance of 8-hydroxyquinoline derivatives for mild steel in acidic medium: Gravimetric, electrochemical, DFT and molecular dynamics simulation investigations. *J. Mol. Liq.* 308 (2020) 113042

[66] L. Toukal, M. Foudia, D. Haffar, N. Aliouane, M. Al-Noaimi, Y. Bellal, H. Elmsellem, I. Abdel-Rahman, Monte Carlo simulation and electrochemical performance corrosion inhibition whid benzimidazole derivative for XC48 steel in 0.5 M H2SO4 and 1.0 M HCl solutions. *J. Indian Chem. Soc.* (2022) 100634

[67] N. I. N. Haris, S. Sobri, Y. A. Yusof, N. K. Kassim, An overview of molecular dynamic simulation for corrosion inhibition of ferrous metals. *Metals,* (2020) 11(1), 46

[68] X. Liu, P. C. Okafor, X. Pan, D. I. Njoku, K. J. Uwakwe, Y. Zheng, Corrosion inhibition and adsorption properties of cerium-amino acid complexes on mild steel in acidic media: experimental and DFT studies. *J. Adhesion. Sci. Tech.* (2020) 1568-5616